Received: 19 October 2018 | Revised: 13 December 2018 | Accepted: 15 January 2019

DOI: 10.1111/ffe.12983

ORIGINAL CONTRIBUTION

WILEY FFEMS Fatigue & Fracture of Engineering Materials & Structures

An online-offline prognosis model for fatigue life prediction under biaxial cyclic loading with overloads

Guoyi Li[1] | Siddhant Datta[1] | Aditi Chattopadhyay[1] | Nagaraja Iyyer[2] | Nam Phan[3]

[1]Arizona State University, Tempe, AZ 85287, USA

[2]Technical Data Analysis Inc., Falls Church, VA 22042, USA

[3]US Naval Air Systems Command, Patuxent River, MD 20670, USA

Correspondence
Guoyi Li, Arizona State University, Tempe, AZ 85287, USA.
Email: guoyili@asu.edu

Funding information
Technical Data Analysis Inc., Grant/Award Number: N68335-16-G-0009, DO 0001; US Navy Naval Air Systems Command

Abstract

This paper presents a robust online-offline model for the prediction of crack propagation under complex in-phase biaxial fatigue loading in the presence of overloads of different magnitudes. The online prognosis model comprises a combination of finite element analysis and data-driven regression to predict the crack propagation under constant loading, while the offline model is trained using experimental data to inform the post-overload crack growth retardation behavior to the online model. The developed methodology is validated by conducting biaxial fatigue experiments using aluminum AA7075-T651 alloy cruciform specimens. A close correlation is observed between the experimental results and model predictions. The results show that the model successfully predicts the crack retardation behavior under the influence of overloads with different magnitudes occurring at different stages of fatigue crack growth. Error analysis is conducted to investigate the sensitivities of the number of training points and crack increments to the prediction accuracy. In addition, the error propagation with respect to the crack length is studied, which provides constructive suggestions for further model improvement.

KEYWORDS

biaxial fatigue, crack propagation, Gaussian process machine learning, online-offline model, overload, prognosis

Nomenclature: a_c, Crack length at current stage; a_f, Crack length at future stage; a_N, Crack length at N^{th} loading cycle; AR_f, Accuracy ratio when crack length is a_f; C_1 & C_2, Coefficients of prognosis model; $\left(\frac{da}{dN}\right)_a$, Acceleration ratio of crack growth rate from $\left(\frac{da}{dN}\right)_{min}$ back to recovery; $\left(\frac{da}{dN}\right)_c$, Crack growth rate at current stage; $\left(\frac{da}{dN}\right)_d$, Deceleration ratio of crack growth rate from overload to $\left(\frac{da}{dN}\right)_{min}$; $\left(\left(\frac{da}{dN}\right)_d\right)_q$, Crack growth rate at retardation region; $\left(\frac{da}{dN}\right)_f$, Crack growth rate at future stage; $\left(\frac{da}{dN}\right)_{min}$, Minimum crack growth rate where crack reaches in retardation due overload; $\left(\frac{da}{dN}\right)_N$, Crack growth rate at N^{th} loading cycle; e_{MAPE}, Mean absolute percentage error; k, Kernel function; K_i, Covariance of training samples; K_p, Covariance of testing samples; K_{ip}, Covariance between training and testing samples; M_S, Material parameter; N_c, Number of fatigue cycle at current stage; N_f, Predicted number of fatigue cycle at future stage; N_{gt}, Ground truth of N_f; N_{NOL}, Fatigue cycle when next overload happens; N_{OL}, Fatigue cycle when current overload happens; R, Stress ratio; S, External load; X, Online training data matrix comprising of input and output parameters; Y, Offline training data matrix comprising of input and output parameters; Z, Normalization constant of posterior distribution; Δa, Crack increment in online-offline framework; ΔK, Stress intensity factor range; ΔK_f, Stress intensity factor range vector of future stage; ΔK_p, Stress intensity factor range vector of testing set; $(\Delta K_{OL})_p$, Stress intensity factor range vector of testing set at instant of overload; λ, Overload ratio; θ, Hyperparameter vector that belongs to the kernel function; μ_1 & μ_2, Mean vectors of input and output posterior distribution, respectively; σ_1^2 & σ_2^2, Variance vectors of input and output posterior distribution, respectively; Φ_i, Offline output parameters of training set; Φ_p, Offline output parameters of testing set

1 | INTRODUCTION

Metallic materials and structures used in mechanical and aerospace applications are subject to complex uniaxial and multiaxial fatigue loading conditions during their service lives.[1] Understanding the crack growth behavior under such complex loading is essential for estimating their useful life and enhancing their operational reliability.[2] The variant induced by load(s), such as single and periodic overload and underload, challenges traditional methodologies in characterizing crack growth mechanisms.[3-5] Hence, a robust model that can accurately predict crack growth rate and fatigue life under complex loading conditions would be highly beneficial for a wide range of structural applications.

To date, there are many experimental and modeling studies devoted to fatigue behavior characterization of metallic materials, with the majority focused on uniaxial and constant loading cases.[6,7] In recent years, understanding and characterizing the crack nucleation and propagation under complex fatigue loading conditions have also seen increased interest. For example, Colin and Fatemi[8] conducted a study to investigate the fatigue behaviors of stainless steel 304L and aluminum AA7075-T6 under step, periodic, and random loadings, which showed that the fatigue life of aluminum AA7075-T6 was affected by overload direction. They found that the tensile overloads resulted in a longer fatigue life, while the compressive overload led to shorter fatigue life. The focus of this study, among many others, was primarily to address issues associated with complex uniaxial loading conditions. A deeper understanding of the behavior of complex structure under biaxial loading conditions with overload, however, remains largely unexplored.

Some early studies[9-11] have shown that the fatigue crack growth rate in the in-plane direction is dependent on the biaxial stress state near the crack tip(s). Recently, the crack growth mechanism of aluminum AA5083-H116[12] was examined under an in-plane biaxial tension-tension fatigue under ambient laboratory and saltwater environments. This research showed that the biaxial loading and the saltwater environment significantly accelerated the crack growth rates in the cruciform specimens. Datta et al[13,14] and Neerukatti et al[15] studied the effect of a single overload on the crack propagation under biaxial loading conditions. The results showed a retardation of crack growth after the overload, and the retardation characteristics exhibited direct dependence on overload ratio and the instantaneous crack length at the occurrence of overload. Although the aforementioned research provided significant insights into the micromechanisms of crack propagation under complex biaxial loading, the accurate prediction of crack propagation in the presence of various overloads and underloads is still an unresolved and challenging issue.

In another study, the fatigue behaviors of aluminum AA7075-T651 was modeled. A mean stress correction-based method was developed for predicting the crack propagation and fatigue life under a very high cycle variable amplitude loading.[16] In addition to the mean stress-dependent approach, a time-based subcycle formulation was developed for predicting fatigue crack growth and crack tip opening displacement under random variable loadings.[17] The formulation was then validated with existing data in the literature and showed impressive capabilities for predicting crack propagation under constant amplitude load with repeated spike overload, spike overload-underload, and continuous overload-underload. An analytical approach[18,19] was also developed for predicting the fatigue crack growth under variable amplitude loading conditions; however, this model is limited to simple geometries.

A micromechanical model has been developed to address the crack initiation under low cycle variable amplitude loading condition for nontraditional geometries.[20] However, the current range of available fatigue life prediction models lack capabilities for predicting damage under complex high cycle loading conditions. One approach to counter this limitation is through use of a recently developed hybrid prognosis algorithm, which is based on a combination of physics-based and data-driven models to predict crack growth under complex biaxial loading conditions.[21] This hybrid model was able to overcome the challenges associated with modeling complex geometries by using physics-based methodologies and the need for large set of training data in data-driven models. In this study, the authors explored the relationship between stress intensity factor (SIF) and crack growth rate for the prediction of crack propagation. The developed model was validated through experiments under a variety of uniaxial fatigue loadings, including constant amplitude loading, constant amplitude loading with overloads, and random loads. The obtained results showed high accuracy with limited training data. The model was later extended to crack prediction under biaxial loading[22]; to address the combination of mode I and II mechanisms near the crack tip under biaxial loading, the energy release rate was used, instead of SIF to explicitly consider these two fracture modes. However, the energy release rate of the cruciform used for biaxial testing could not be calculated analytically due to the complex geometry. Therefore, a regression model based on Gaussian process machine learning was developed to explore the nonlinear relationship between energy release rate and the different crack tip locations in the cruciform.[23] This

framework was validated through biaxial experiments on aluminum AA7075-T651 aluminum alloy under various loading conditions.

In this paper, the previously mentioned hybrid methodology is further extended as an online-offline prognosis framework for predicting nonlinear crack propagation in aluminum AA7075-T651 cruciform specimens under biaxial loading conditions in the presence of overload. The online model is trained by training points from a real-time test for crack propagation prediction, while the offline model is trained by existing experimental data and will provide the physics-based parameters to the online model in the proposed research. The influence of a single overload on the crack propagation behavior is studied taking into consideration different magnitudes and occurrences at different stages of fatigue crack growths, approximately 3 to 10 mm in this study. The crack propagation under constant biaxial loading is predicted using the originally developed prognosis model. Three additional physics-based parameters—minimum crack growth rate, crack growth retardation rate, and crack growth acceleration rate—are introduced to address the nonlinearity in crack growth due to the presence of overload, in particular, crack retardation due to overload. These parameters govern crack retardation behavior and are obtained through biaxial tension-tension experiments under overloads with different overload ratios, and the relationships between these parameters and the SIF range under overloads are modeled using the Gaussian process as an offline model. The developed framework is validated through biaxial experiments conducted with single overloads of different overload ratios, including the situation of two overloads in a single test. The predicted crack propagation behaviors showed good agreement with the experiments.

The remainder of this paper is organized as follows. A detailed formulation of the proposed online-offline model is presented in Section 2. This is followed by a description of the experimental procedure (including cruciform specimen design and test procedure) and the results in Section 3. The results from the prognosis model on crack propagation under biaxial loading with overloads including a comprehensive error analysis are presented in Section 4. Key observations from this work are summarized in the concluding remarks section.

2 | ONLINE-OFFLINE PROGNOSIS MODEL

This section presents the development of the prognosis formulations for predicting crack length with respect to loading cycle. A limited number of training points comprising crack length with respect to loading cycle data in early stage-II crack propagation region are used. The online-offline model described here is expected to predict crack growth retardation after the overloads based on the information including the instant of overloads and overload ratios. A previously developed hybrid prognosis model[22] is modified here as an online model for predicting crack growth in real time. However, this model has also shown an obvious underprediction of crack length at a certain fatigue cycle under uniaxial loading with overloads; such an inaccuracy can increase the risks of structural failure risk (type-II error).[21] To handle the retardation effects due to overloads, therefore, additional knowledge is necessary to inform this online model for improved prediction. Based on this, an offline prognosis model can be developed as well as integrated into the online model, as shown in Figure 1. In a real experiment, the online model is able to predict crack growth under the in-phase constant biaxial loading, ie, at the instant of an overload, the developed offline model simulates the crack growth behavior using the three physics-based variables, which are trained using experimental data. Once the effect of overload on crack growth behavior diminishes, the online model is then used to predict the crack growth. The detailed formulations are included in the next two subsections.

2.1 | Online model

The online model was originally derived by the authors' group (Neerukatti et al[21,22]) and is briefly explained here for the sake of completeness. In the following formulations, the log sign represents the natural logarithm. The crack growth rate $\left(\frac{da}{dN}\right)_N$, at N^{th} loading cycle with a crack length a_N, is written as

$$\log\left(\frac{da}{dN}\right)_N = C_1\left(a_N, M_s, S_{N,N+1}, N\right) + C_2\left(a_N, M_s, S_{N,N+1}, N\right)\log(\Delta K_N) \quad (1)$$

where M_S is a material parameter, S is the load, and ΔK, which can be expressed as $\Delta K = K_{max} - K_{min}$, is the SIF range. In this study, as shown later in Section 3, the in-phase proportional cyclic loading results in a 45° crack propagation direction under a pure mode-I stress-state; as such, the ΔK specifically represents the mode I SIF range. However, due to the complex nature of fatigue crack growth after an overload, as reported in previous studies,[13,15] the uncertainty of the inference from $log(\Delta K)$ to $\log\left(\frac{da}{dN}\right)$ has to be considered; note that the uncertainties from the coefficients C_1 and C_2 that are included

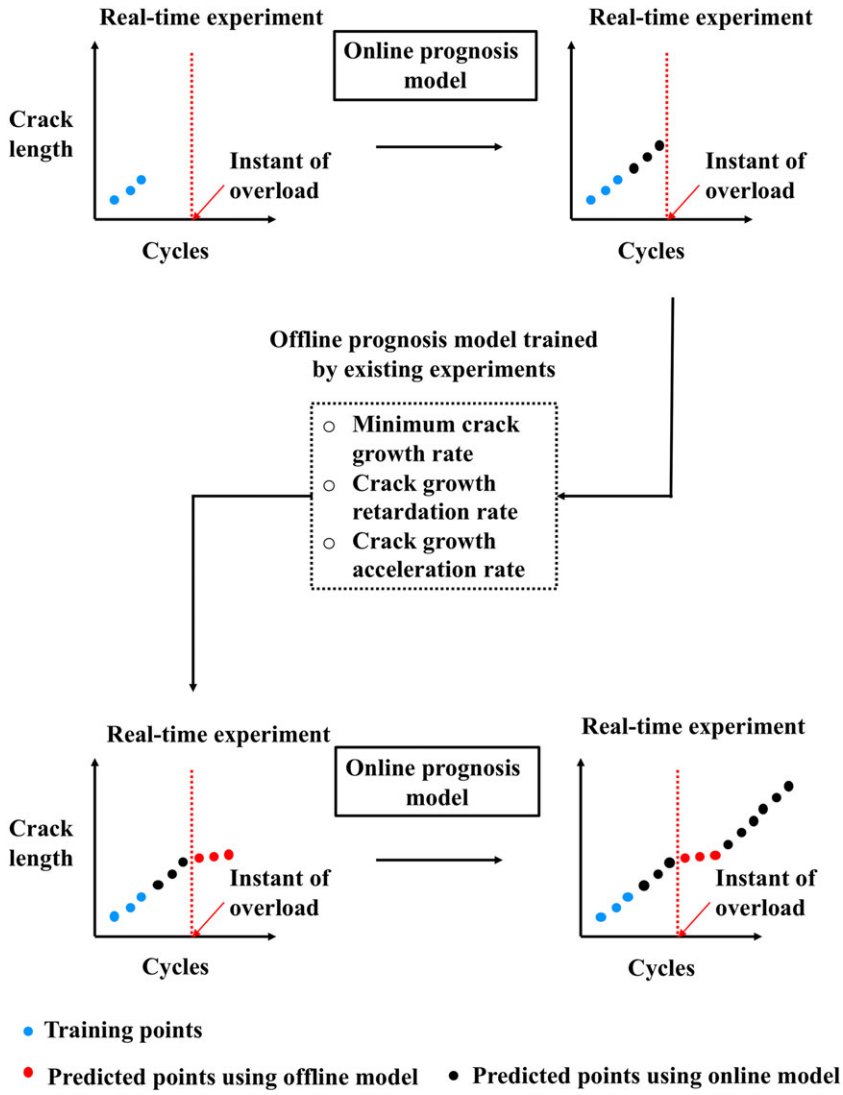

FIGURE 1 A demonstration of the developed online-offline prognosis model [Colour figure can be viewed at wileyonlinelibrary.com]

in Equation 1. In order to investigate the effects of training information on prediction uncertainties in crack propagation at a relatively large crack length, especially after overloads, this prognosis model is formulated as a Gaussian process learning model based on a Bayesian inference strategy developed by Rasmussen and Williams.[23] The posterior distribution is expressed as follows:

$$f\left(\log\left(\frac{da}{dN}\right)_p | X, \Delta K_p, k, \theta\right) = \frac{1}{Z}\exp\left(-\frac{\left(\log\left(\frac{da}{dN}\right)_p - \mu_1\right)^2}{2\sigma_1^2}\right) \quad (2)$$

where k is the kernel function (also known as covariance function), $X = \{log\Delta K_i,\ \log\left(\left(\frac{da}{dN}\right)_i\right)\}$ is the training matrix comprising the input parameter ΔK and the output parameter $\frac{da}{dN}$, ΔK_p is the input of the testing set, Z is a normalization constant, and θ is the hyperparameter vector that belongs to the kernel function. For simplification, in the rest of this paper, K_i denotes the covariance of the training samples $k(log(\Delta K_i), \log(\Delta K_j))$, K_p denotes the covariance of testing samples $k(log(\Delta K_p), log(\Delta K_p))$, and K_{ip} denotes the covariance between training and testing samples $k(\log(\Delta K_p), \log(\Delta K_i))$. Therefore, the mean $\mu_1$and variance of the distribution σ_1^2 are obtained as

$$\mu_1 = K_{ip}K_i^{-1}\log\left(\Delta K_p\right) \quad (3a)$$

and

$$\sigma_1^2 = K_p - K_{ip}K_i^{-1}K_{ip}^T \quad (3b)$$

where subscripts $i, j = 1, 2, ..., (n-1)$ denote the training points, and the subscript $p = n, (n+1), ..., m$ represents the prediction points. As indicated by Rasmussen and Williams, the accuracy of the prediction depends on the choice of the kernel functions and their hyperparameters.

The squared exponential (SE) kernel function, which is one of the most widely accepted kernels, showed robustness in modeling a nonlinear smooth surface with a high prediction accuracy[21,22] and is used in this work. The SE kernel can be expressed as

$$k(x_i, x_j) = \theta_1^2 \exp\left(\frac{(x_i - x_j)^2}{\theta_2^2}\right) \quad (4)$$

where the hyperparameter vector can be defined as $\theta = [\theta_1\ \theta_2]$. The θ can be tuned using known *maximum a posteriori* (MAP) estimation through the negative logarithmic marginal likelihood function, which can be expressed as

$$-\frac{1}{2}K_{ip}^T K_i^{-1} K_{ip} - \frac{1}{2}\log|K_i| - \frac{m-n+1}{2}\log 2\pi. \quad (5)$$

Using the optimal hyperparameter vector, the crack growth rate can be found through the inference with a known ΔK. It should be noted that the inference in this model is in a logarithmic scale, unlike the formulations in the originally developed method. The primary reason is that a large magnitude difference between ΔK and $\frac{da}{dN}$ results in a relatively large prediction error, especially after the occurrence of overload. Consequently, prediction in logarithmic scale, which reduces the magnitude difference, can improve the accuracy.

A second Gaussian process regression model is used for predicting the SIF range under in-phase loading in order to obtain the value of ΔK at a specific crack length; detailed information can be found in Neerukatti et al.[22] In this research, the Gaussian process model is used to find the ΔK corresponding to fracture mode I instead of the energy release rate. By implementing this model, the ΔK_f can be found through the crack length a_f, which is larger than the current crack length a_c at fatigue cycle N_c. Therefore, $\left(\frac{da}{dN}\right)_f$ can be computed using Equation 1, and the fatigue cycle N_f corresponding to a_f can be expressed as

$$N_f = N_c + \frac{\Delta a}{\left(\frac{da}{dN}\right)_f} \quad (6)$$

where $\Delta a = a_f - a_c$, which represents the assumed crack increment.

2.2 | Offline model

The offline model is developed for predicting the crack growth after the instant of overload. Based on the experimental observations,[13] it is hypothesized that the crack growth rate experiences a retardation after a single overload and gradually recovers to the steady-state crack growth rate in the absence of an overload. To statistically model this behavior, three variables are introduced based on this hypothesis: minimum crack growth rate, crack growth retardation rate, and crack growth acceleration rate in logarithmic scale. As shown in Figure 2, the minimum crack growth rate, $\left(\frac{da}{dN}\right)_{min}$, represents the minimum growth rate in the crack retardation process after the instant of an overload; the crack growth retardation rate, $\left(\frac{\dot{da}}{dN}\right)_d$, is the deceleration ratio of the crack growth rate from the instant of an overload to the $\left(\frac{da}{dN}\right)_{min}$; and the crack growth acceleration rate, $\left(\frac{\dot{da}}{dN}\right)_a$, denotes the acceleration ratio of crack growth rate from $\left(\frac{da}{dN}\right)_{min}$ back to the steady-state crack growth rate, which is defined as the instant of recovery.

In order to avoid an unwieldy formulation, these variables are expressed in vector form as,

$$\Phi = \left\{ \log\left(\frac{da}{dN}\right)_{min}, \log\left(\frac{\dot{da}}{dN}\right)_d, \log\left(\frac{\dot{da}}{dN}\right)_a \right\}. \quad (7)$$

As in the online model, Φ_i denotes the vector of training set and Φ_p represents the output vector of the testing set. The Gaussian process model is used to model the behaviors of crack growth in the overload region and is expressed as follows:

$$f\left(\Phi_p | Y, (\Delta K_{OL})_p, k, \theta\right) = \frac{1}{W}\exp\left(-\frac{(\Phi_p - \mu_2)^2}{2\sigma_2^2}\right) \quad (8)$$

where $Y = \{(\Delta K_{OL})_i, \Phi_i\}$ is the training matrix comprising the input parameter $(\Delta K_{OL})_i$ and the output parameter Φ_i, $(\Delta K_{OL})_p$ is the input of the testing set, W is a

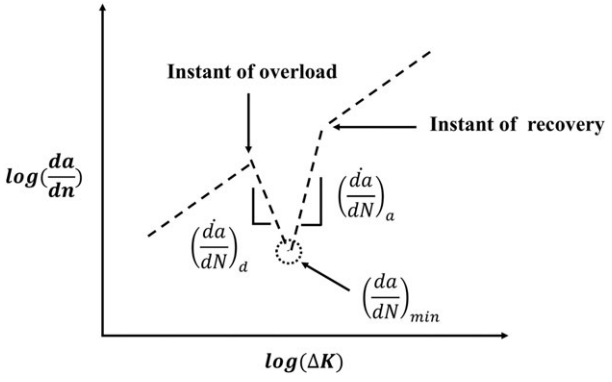

FIGURE 2 Schematic of the three defined variables that govern the crack propagation after overload

normalization constant, and each row of θ is the hyperparameter corresponding to a specific output variable in Φ. Because the SE kernel k is also utilized in this model due to its aforementioned capability, θ can be expressed as

$$\theta = \begin{bmatrix} [\theta_1\ \theta_2]_{min} \\ [\theta_1\ \theta_2]_d \\ [\theta_1\ \theta_2]_a \end{bmatrix} \tag{9}$$

where $[\theta_1\ \theta_2]_{min}$, $[\theta_1\ \theta_2]_d$, and $[\theta_1\ \theta_2]_a$, which are obtained using a MAP estimation described in Equation 5, are the hyperparameters corresponding to $\log\left(\frac{da}{dN}\right)_{min}$, $\log\left(\frac{\dot{da}}{dN}\right)_d$, and $\log\left(\frac{\dot{da}}{dN}\right)_a$, respectively. It is worth mentioning that the input of this model is defined as the SIF range at the instant of overload, ΔK_{OL}, because the behavior of the crack growth highly depends on the overload ratio. The hypothesis made here is that these three variables are governed by the SIF range at the instant of overload, ΔK_{OL}, which can also be found through the aforementioned model.[22] Statistically speaking, the choice of ΔK_{OL} fuses the information of ΔK with the overload ratio, further correlating the behavior of crack growth with the overload ratio in addition to ΔK. Therefore, for the q^{th} crack increment Δa, where $\Delta a = a_q - a_{q-1}$, the crack growth rate $\left(\left(\frac{da}{dN}\right)_d\right)_q$ at the retardation region can be expressed as

$$\left(\left(\frac{da}{dN}\right)_d\right)_q = \exp\left(\log\left(\left(\frac{da}{dN}\right)_d\right)_0 + \log\left(\frac{(\Delta K_{OL})_q}{(\Delta K_{OL})_{q-1}}\right)\log\left(\left(\frac{\dot{da}}{dN}\right)_d\right)\right) \tag{10}$$

where $\left(\left(\frac{da}{dN}\right)_d\right)_0$ is the crack growth rate at the instant of the overload. Equation 10 governs the crack growth until the crack growth rate reaches the minimum value obtained through the developed model, ie, $\left(\left(\frac{da}{dN}\right)_d\right)_q \le \left(\frac{da}{dN}\right)_{min}$. Following this, the crack will experience crack growth rate acceleration, and the crack growth rate $\left(\left(\frac{da}{dN}\right)_a\right)_q$ can be expressed as follows:

$$\left(\left(\frac{da}{dN}\right)_a\right)_q = \exp\left(\log\left(\left(\frac{da}{dN}\right)_{min}\right) + \log\left(\frac{(\Delta K_{OL})_q}{(\Delta K_{OL})_{q-1}}\right)\log\left(\left(\frac{\dot{da}}{dN}\right)_a\right)\right). \tag{11}$$

The crack growth rate will accelerate till the steady-state crack growth rate in the absence of an overload is reached, ie, $\left(\left(\frac{da}{dN}\right)_a\right)_q \ge \left(\frac{da}{dN}\right)_q$.

By merging the developed online and offline models for crack propagation under in-phase biaxial loading with a single overload at a known fatigue cycle N_{OL}, the fatigue life cycle N_f can be obtained as follows:

$$N_f = N_c + \frac{\Delta a}{\left(\frac{da}{dN}\right)_f};\ if\ N_c \le N_{OL} \tag{12a}$$

$$N_f = N_c + \frac{\Delta a}{\left(\frac{da}{dN}\right)_d};\ if\ N_c \ge N_{OL} \& \left(\left(\frac{da}{dN}\right)_d\right)_f \ge \left(\frac{da}{dN}\right)_{min} \tag{12b}$$

$$N_f = N_c + \frac{\Delta a}{\left(\frac{da}{dN}\right)_a};\ if\ N_c \ge N_{OL} \& \left(\left(\frac{da}{dN}\right)_d\right)_f \le \left(\left(\frac{da}{dN}\right)_a\right)_f \le \left(\frac{da}{dN}\right)_f \tag{12c}$$

$$N_f = N_c + \frac{\Delta a}{\left(\frac{da}{dN}\right)_f};\ if\ N_{OL} \le N_c \le N_{NOL} \& \left(\left(\frac{da}{dN}\right)_a\right)_f \ge \left(\frac{da}{dN}\right)_f \tag{12d}$$

where Δa, a_c, and a_f are the crack increment, the current crack length, and the predicted crack length, respectively. N_{NOL} denotes the instant of next overload, if there is. It should be noted that the Equation 12a to 12d represent the assumptions made in the developed model: (1) the overload leads to a crack growth retardation, but it has negligible impact on the crack propagation after the instant of recovery; (2) in the event of multiple overloads, the time between two overloads is long enough so that the effect of the first overload on the second overload can be ignored.

For comparing the prediction error with different crack increments Δa and training set, the widely used error measurement model, ie, mean absolute percentage error (MAPE),[24] is implemented, which can be expressed as

$$e_{MAPE} = \frac{1}{M}\sum_{j=1}^{M}\left|\frac{(N_{gt})_j - (N_f)_j}{(N_{gt})_j}\right| \tag{13}$$

where M is the total number of predicted points in a single test, ie, $M = m - n + 1$, and N_{gt} is the ground truth that comes from an actual experiment. However, as mentioned by Tofallis,[25] this method is no longer feasible for the investigation of error propagation with respect to the crack length in a single test due to its biased characteristics. Therefore, logarithmic accuracy ratio (AR)[25,26] is implemented for the analysis of error propagation within a single test, and the formulation is expressed as

$$AR_f = \log\left(\frac{N_f}{(N_{gt})_f}\right) \tag{14}$$

where AR_f is the logarithmic AR when crack length is a_f while the predicted fatigue cycle is $(N_{gt})_f$. Because the predicted data are strictly positive, this method is well suited in the current study; it provides quantitative information of error propagation with respect to crack length, as well as a distinguishable visualization of both underprediction and overprediction.

3 | BIAXIAL FATIGUE EXPERIMENT

The crack propagation behavior of aluminum AA7075-T651 was investigated in this research as a validation of the developed prognosis model; biaxial tension-tension fatigue tests were conducted under in-phase loading with single overloads with biaxiality ratio of 1.0. An MTS biaxial/torsion load frame with a capacity of 100-kN planar bi-axial and 1100 N-m torsion, equipped with six independent controllers, was used for the fatigue testing. Fatigue tests were conducted with stress-control load spectra having single overloads interspersed in an otherwise constant amplitude baseline fatigue loading. To analyze the effect of different overload magnitudes on crack growth behavior, tests were conducted with overload ratios λ of 1.75, 2, and 2.25. The overload ratio was defined as the ratio of maximum load at the instant of overload to the maximum load of the constant amplitude cycles. Biaxial fatigue load spectra with a frequency of 10 Hz were generated with single overload excursions after a pre-decided number of 1.5 to 15-kN constant amplitude fatigue cycles, resulting in a stress ratio R of 0.1 in both vertical and horizontal directions. The samples were machined using 6.35-mm rolled aluminum AA7075-T651 sheets with the thickness of web area being 1.8 mm as shown in Figure 3. The length and width of the arms were 292 and 48.35 mm, respectively. First, a hole of diameter 6.35 mm was cut at the center of the web area, and then a notch of length 1.5 mm and width 0.36 mm was made at an angle of 45° to the horizontal and vertical directions to (1) enforce the location of crack initiation at a desired location and (2) accelerate the crack initiation to feasibly study crack propagation behavior. Figure 4 shows the biaxial fatigue test setup. The crack length was measured using a digital image correlation system (ARAMIS) along with a high-resolution optical camera. For in-phase loading, it was observed that a single crack initiates and propagates perpendicular to the maximum normal stress direction, ie, at an angle of approximately 45° to the loading directions, because the load is equal along horizontal and vertical directions, and propagation along this direction maximizes the mode-I SIF.

From the biaxial fatigue experiments with single overloads,[13] it was observed that the occurrence of overload during crack propagation results in immediate and drastic reduction in crack growth rate. Following this, the crack growth recovers gradually as the crack-tip propagates further and extends past the overload affected region. The region of crack propagation, where reduced crack growth rate was observed, is referred to as the retardation zone, and the size of the retardation zone was found to be directly proportional to the λ of the overload. Overloads with higher λ lead to larger plastic zones

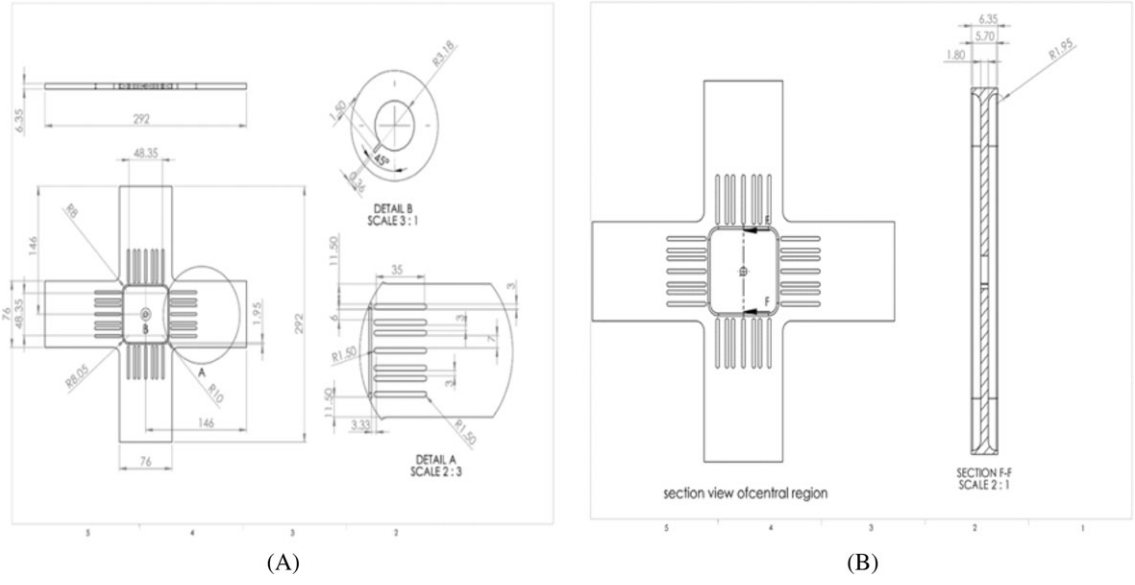

FIGURE 3 Cruciform specimen design used for biaxial fatigue testing

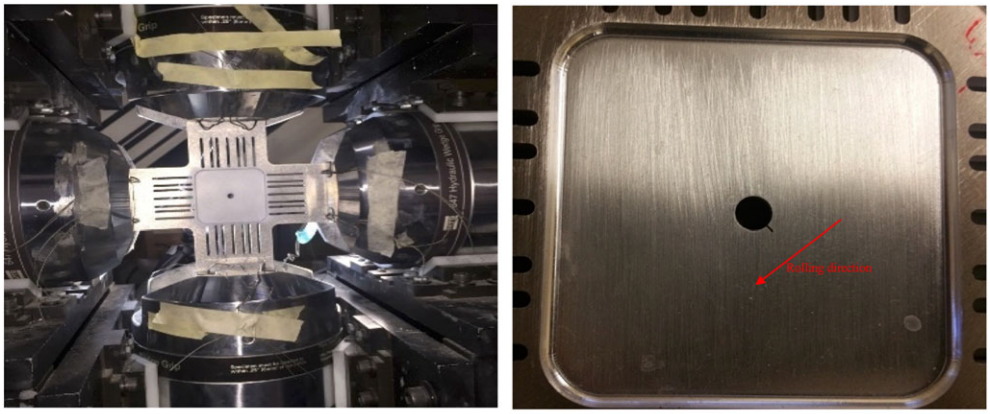

FIGURE 4 Biaxial fatigue test setup for aluminum AA7075-T651 cruciform: A, cruciform specimen in the biaxial test frame; B, web area of cruciform with notch [Colour figure can be viewed at wileyonlinelibrary.com]

around the crack-tip, causing increased plasticity-induced crack closure on the crack, which in-turn severely retards the crack growth. Another interesting observation from the experimental results indicated that the retardation effects were more pronounced when overload occurs at a larger crack length, and the post-overload crack-tip traverses a longer distance before the crack growth rate recovers to values comparable to the steady rate. This is also attributed to the increased plasticity-induced crack closure due to overload occurrence at a large crack length, because the crack-tip plastic zone size is directly proportional to crack length and load magnitude. The hypotheses and assumptions made in the developed model, which are mentioned in Section 2, are based on these experimental observations.

4 | RESULT AND DISCUSSION

This section presents the results and discussions from the developed prognosis model. First, the training processes and corresponding results are discussed, followed by a discussion on the developed offline model. The performance of the online-offline model is investigated with respect to crack increment Δa and the number of training points. Prognosis results are presented for various scenarios that include different overload ratios and several overloads in a single test. This is followed by a comprehensive error analysis.

4.1 | Model training

The geometry of the cruciform structure shown in Figure 3 is explicitly modeled; a total of 216 simulations with different combinations of loads and crack tip locations were performed using the commercial finite element solver Abaqus.[27] An accurate mapping from the four-parameter input (vertical and horizontal crack tip locations and loads) to ΔK is established using the introduced Gaussian process learning method.[22] As the real fatigue tests proceed, the full fatigue life is predicted using the developed online model based on the limited data (cycle with respect to crack length).

In addition to the online model, the offline model is used for all the test cases as a priori knowledge of the online model. The experiments performed for offline model training are summarized in Table 1; for each test,

TABLE 1 Summary of the tests performed for offline model training

Test	Overload Ratio	Instant of Overload	Crack Length when Overload Applied [mm]	Cycles to Failure
1	1.75	30 000	3.76	75 600
2	1.75	45 000	4.75	108 300
3	2.0	30 000	6.77	63 300
4	2.0	60 000	8.32	99 700
5	2.25 2.25	30 000 80 000	3.00 10.73	140 100 140 100

the minimum crack growth rate $\left(\frac{da}{dN}\right)_{min}$, crack growth retardation rate $\left(\frac{\dot{da}}{dN}\right)_d$, and crack growth acceleration rate $\left(\frac{\dot{da}}{dN}\right)_a$ are calculated, and the corresponding ΔK_{OL} is obtained using the locations of crack tip and the loads, forming the training set Y. Consequently, for any new crack length, the corresponding vector Φ_p can be obtained through Equation 8 using the testing set $(\Delta K_{OL})_p$. The crack growth behavior is then predicted using Equations 10 and 11.

Figure 5A-C presents the results of the minimum crack growth rate $\left(\frac{da}{dN}\right)_{min}$, crack growth rate deceleration, and acceleration, respectively, with their 95% confidence intervals. In these figures, the range of prediction is larger than the training set for better visualization of the nonlinear behavior. In addition, the logarithmic scale and feature normalization is used because the accuracy and learning speed of MAP estimation are improved by scaling the input Φ and output ΔK_{OL} into a domain where all features have similar scale.[28] As shown in Figure 5, the values of $\left(\frac{da}{dN}\right)_{min}$, $\left(\frac{\dot{da}}{dN}\right)_d$, and $\left(\frac{\dot{da}}{dN}\right)_a$ reduce with increase in ΔK_{OL}. As seen from these figures, the uncertainty associated with the offline model is small in the region near the training data, and the prediction confidence reduces when testing points are far from the training points. It should be noted that the tests mentioned in this subsection are used for training only; the evaluation and validation of the developed model are conducted using completely different tests and are presented next.

4.2 | Model evaluation

The developed model contains two parameters, the number of training points and crack increment Δa, that were not included in the optimization scheme and must be investigated. Before model evaluation, it is necessary to mention the definitions of underprediction and overprediction in this study. When the model predicts a larger number of cycles than the actual number of cycles at a certain crack length, it is regarded as an overprediction; in this case, the crack length from the model is shorter than the actual crack length, which is equivalent to an underprediction of crack length. The model undergoes an underprediction if it predicts a smaller number of cycles than the actual number of cycles at a certain crack length; in this case, the crack length from the model is larger than the actual crack length, which is equivalent to an overprediction of crack length. It is slightly different from the general definitions, because the developed model mathematically predicts the increment of fatigue cycles with a certain crack increment as mentioned before. In this section, with the hypothesis that the effects of Δa and number of training points on the prediction accuracy are independent, the prognosis results of a test

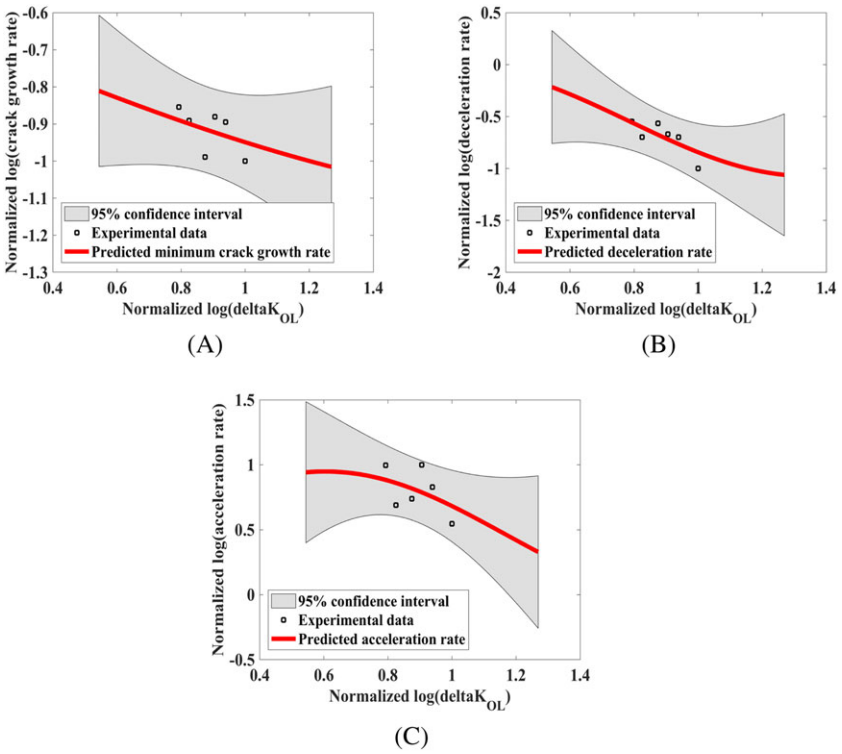

FIGURE 5 Offline model of normalized logarithmic: A, minimum crack growth rate; B, deceleration; and C, acceleration of crack growth after an overload [Colour figure can be viewed at wileyonlinelibrary.com]

with the instant of overload at cycle of 25 000 (overload ratio equals to 1.75) are discussed in this subsection to show the sensitivities of these two parameters while serving as one of the validation tests. It should be noticed that this hypothesis will be investigated and further proved in this section.

4.2.1 | Convergence with respect to the number of training points

The sensitivity of the prediction with respect to the number of training points is essential to the developed prognosis model, and it is evaluated in this subsection. Maintaining the crack increment Δa to be 0.01, Figures 6 and 7 show the prediction of the crack growth rate and the fatigue cycle, respectively, using different number of training points. It is seen that the predicted crack propagation behavior is very similar to the actual experiments starting with three training examples. It indicates that the Gaussian process learning model cannot model the behaviors of $\log\left(\frac{da}{dN}\right)$ with respect to $\log(\Delta K)$ with only two or less training points in the current study. Consequently, the inaccuracy in predicting behavior of $\log\left(\frac{da}{dN}\right)$ with respect to $\log(\Delta K)$ before the overload using two training examples results in a large offset when predicting the later overload region, as shown in Figure 7 A, due to the coupled governing equations of the constant and overload regions, shown in Equation 12. When the confidence intervals obtained from the model trained by different number of training points are compared, a 95% confidence interval becomes narrow with respect to the increased training set size, indicating more confidence in the prediction that has more training examples.

The MAPE of the prediction with respect to the number of training points is shown in Figure 8. It can be seen that the MAPE decreases rapidly and then converges to a certain value, 0.05 (5%) in this case. At this point, two clarifications need to be mentioned: First, the number of observations in this case is up to eight only. The reason is that the maximum number of training points is not guaranteed due to the crack initiation after different numbers of cycles in different tests, and the overload is applied at the ninth experimental data point in this test. However, the robustness of the developed online-offline model cannot be convincingly demonstrated, if the overload information ($\left(\frac{da}{dN}\right)_{min}$, $\left(\frac{\dot{da}}{dN}\right)_d$, and $\left(\frac{\dot{da}}{dN}\right)_a$) of the current experiment is provided to the developed model. Based on this consideration, the purpose of studying and showing the convergence of the prediction error with respect to the number of training points is to demonstrate that the developed model can predict the crack propagation accurately using very limited amount of training information. For a realistic application, if the overload region is already known, the crack propagation can be predicted just using the online model. Second, variations of MAPE can be seen when the model is trained by three

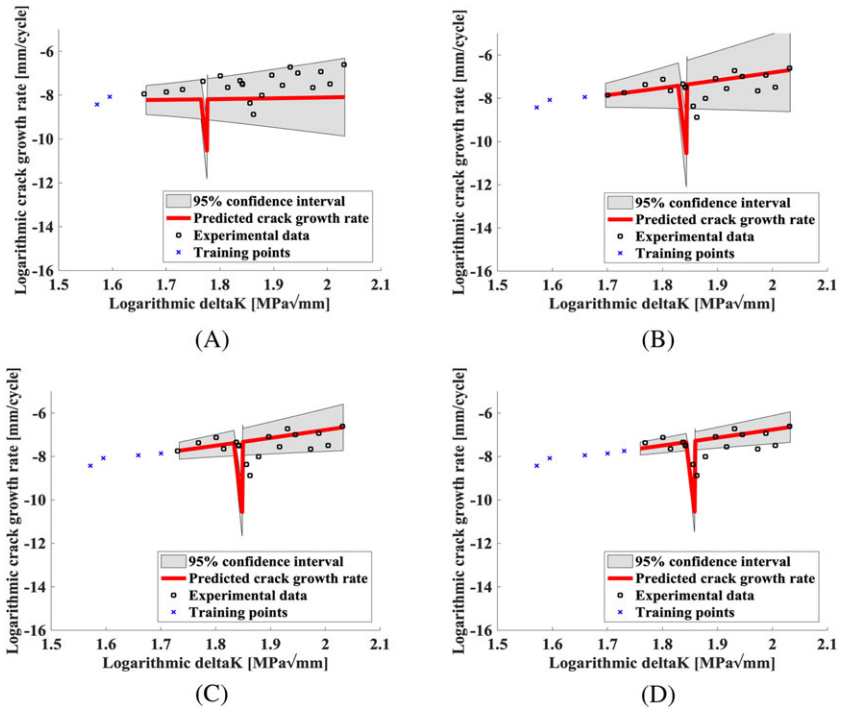

FIGURE 6 Predictions of the crack growth rate with respect to SIF range using A, 2; B, 3; C, 4; and D, 5 training examples [Colour figure can be viewed at wileyonlinelibrary.com]

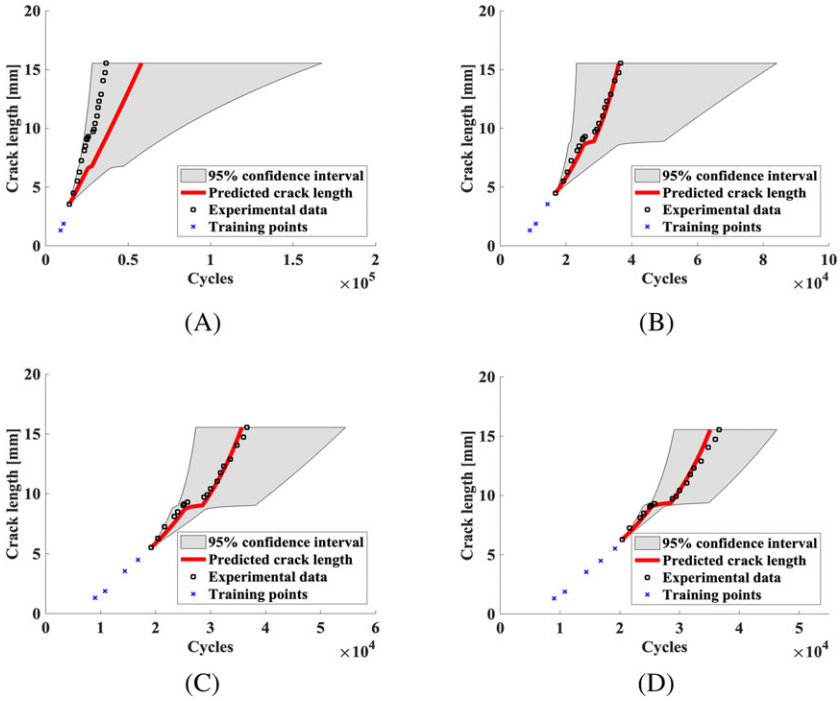

FIGURE 7 Predictions of the crack propagation with an overload at the cycle of 25 000 using A, 2; B, 3; C, 4; and D, 5 training examples [Colour figure can be viewed at wileyonlinelibrary.com]

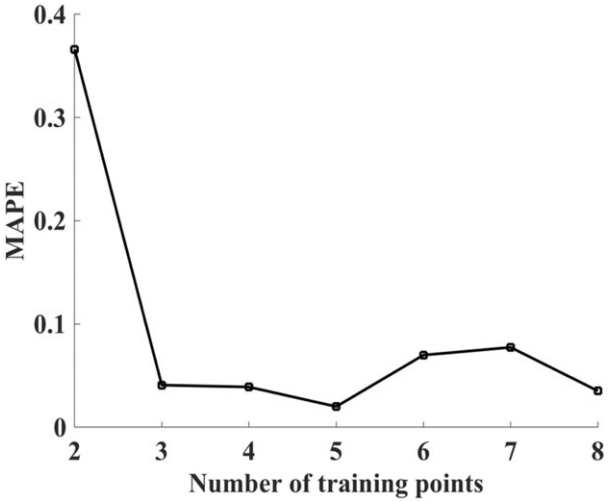

FIGURE 8 MAPE of the prediction with respect to the number of training points

or more data points. The reasons, which result in the unavoidable prediction variation, are as follows: (1) the developed model predicts the number of fatigue cycles using a certain crack increment, and the scale of the fatigue cycle is significantly larger than the crack length, resulting in high sensitivity to the variations of crack growth rate; (2) due to the data-driven nature, the accuracy of developed model depends on the experimental observations that contain uncertainties, which results in a slight increase of MAPE when number of training samples is above five in this particular case.

4.2.2 | Convergence with respect to crack increment Δa

The sensitivity of the developed model to the crack increment Δa is investigated using the same test as discussed in the previous subsection; in this study, the number of training points are set to be five, as it can provide a reliable crack propagation behavior. The value of Δa is varied from 0.001 to 1 mm; the MAPEs of all the cases are computed.

Figures 9 and 10 show the prediction of the crack growth rate and the fatigue cycle, respectively, using different values of Δa. It is seen that the model slightly overpredicts the crack propagation behavior when the value of Δa is 0.1. When Δa equals to 0.01 or 0.001, the model can predict the crack growth with high accuracy. From Figure 9A to D, it can be observed that the value of Δa has a huge impact on the prediction accuracy of the crack growth behavior at the overload region. The interpretation is that a large Δa might result in a large fatigue cycle increment right before the overload and lead to a large overprediction as shown in Figure 10A,B. Comparing Figure 10C,D, it is seen that the prediction will be almost identical. In addition, the size of confidence interval decreases with the decrease of Δa.

Next, the correlation between number of training points and Δa is investigated as shown in Figure 11. It can be seen that the prediction accuracy is large when Δa equals to 0.5, irrespective of the number of experimental points used to train the model. However, when

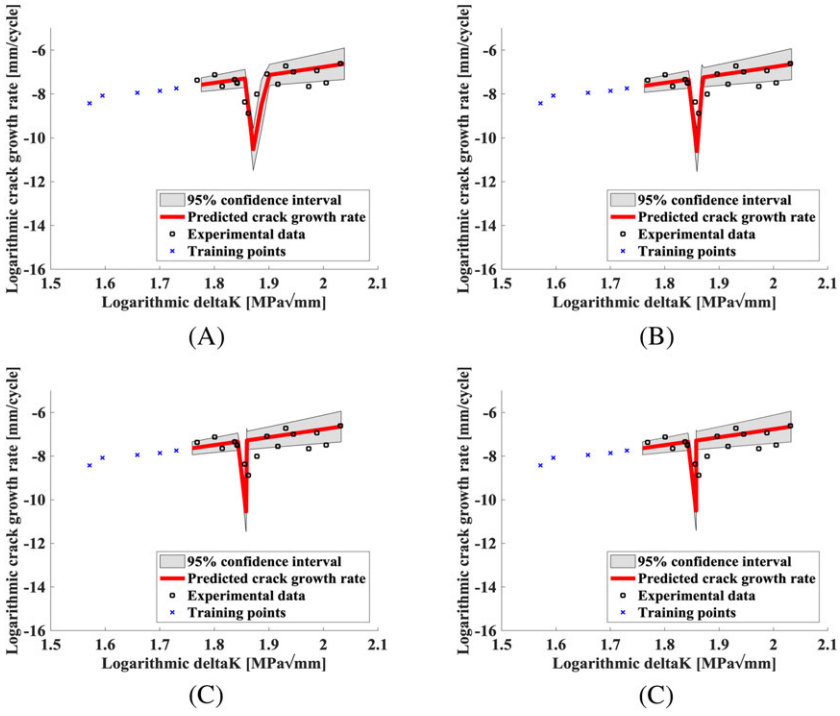

FIGURE 9 Predictions of the crack growth rate when the value of Δa equals to A, 0.5; B, 0.1; C, 0.01; and D, 0.001 [Colour figure can be viewed at wileyonlinelibrary.com]

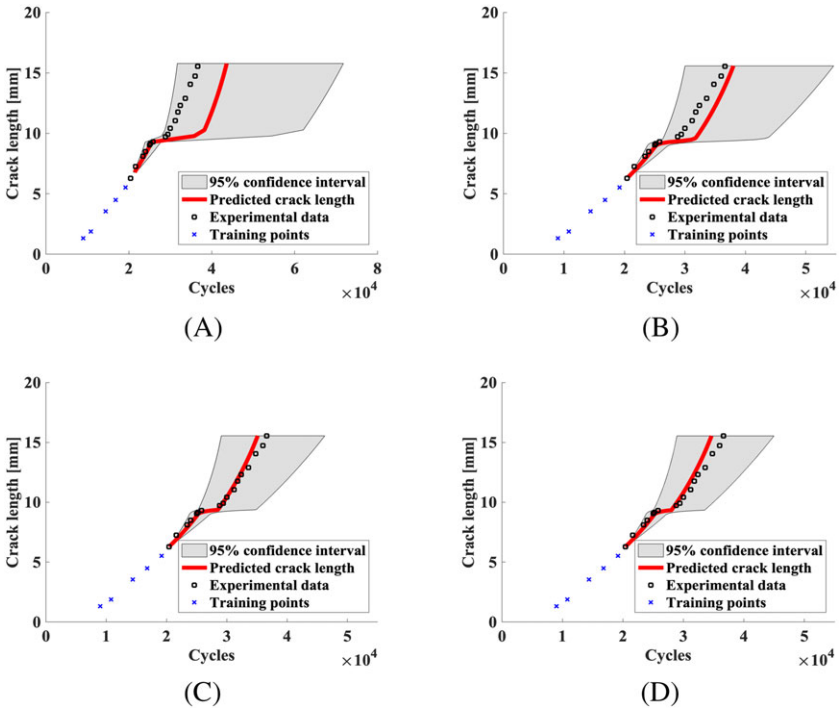

FIGURE 10 Predictions of the crack propagation with an overload at the cycle of 25 000 when the value of Δa equals to A, 0.5; B, 0.1; C, 0.01; and D, 0.001 [Colour figure can be viewed at wileyonlinelibrary.com]

Δa is small enough, ie, $\Delta a \leq 0.1$, the prediction error follows the same tendency, and the prediction errors, when $\Delta a = 0.01$ and $\Delta a = 0.001$, are almost identical. In addition, for a certain number of training points, the accuracies are close to each other. This observation proves the hypothesis that the number of training points and Δa are independent, when the Δa is small enough.

4.3 | Prognosis results under various overload conditions

In this section, the developed model is used for predicting the crack propagation under different values of overload ratios and investigating the case that contains two overloads in a single test. The prognosis results of a test with

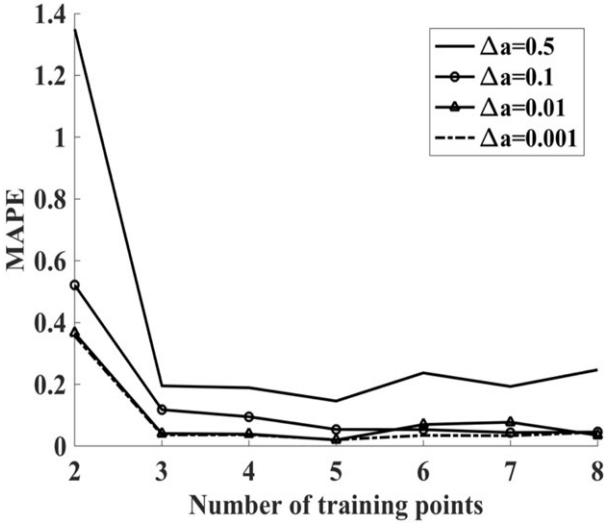

FIGURE 11 Investigation of the independence between the number of training point and Δa

the instant of overload at 30 000 fatigue cycles (overload ratio equals to 2.0) are presented in Figure 12; based on the observation in model evaluation, the number of training samples and the crack increment, Δa, are set to be 5 and 0.01, respectively. It can be observed that the developed model precisely predicts the crack growth of the experimental sample, which proves its robustness in predicting crack propagation under different overload ratios.

Next, the prognosis results of a test with the instants of overload at 30 000 and 45 000 fatigue cycles (overload ratio equals to 1.75) are presented in Figure 13; similar to the previous case, the number of training samples and the crack increment Δa are set to be 3 and 0.01, respectively. The reason for using less training points in this case is that the total number of observations before the first overload is limited (five points) from the experiments. As mentioned before, to show the robustness of both online and offline model, a relatively smaller number of training points are chosen. It can be seen that the developed model successfully predicts the crack growth of the experimental sample, which proves the capability of the developed model in predicting crack propagation with the overloads in a single test. Comparing with the test containing only one overload, a relatively larger underprediction can be found, especially after the first overload. In details, due to the underprediction of the crack growth between two overload regions, a delay of prediction is observed in predicting the retardation that resulted from the second overload, which is clearly demonstrated in Figure 13A. In order to obtain the insights of such issues, an error analysis is performed to investigate how and why the prediction error evolves with respect to the crack propagation.

4.4 | Discussion of error propagation with respect to crack length

A logarithmic AR error analysis is used for investigating the propagation of prediction error with respect to the

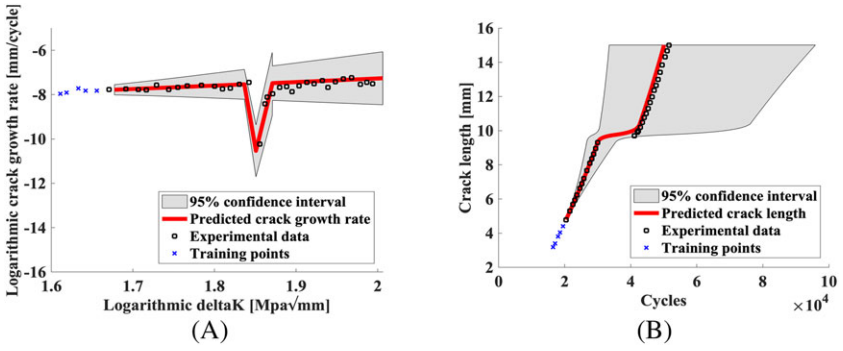

FIGURE 12 Predictions of the crack growth rate and crack propagation with an overload ratio of 2.0 [Colour figure can be viewed at wileyonlinelibrary.com]

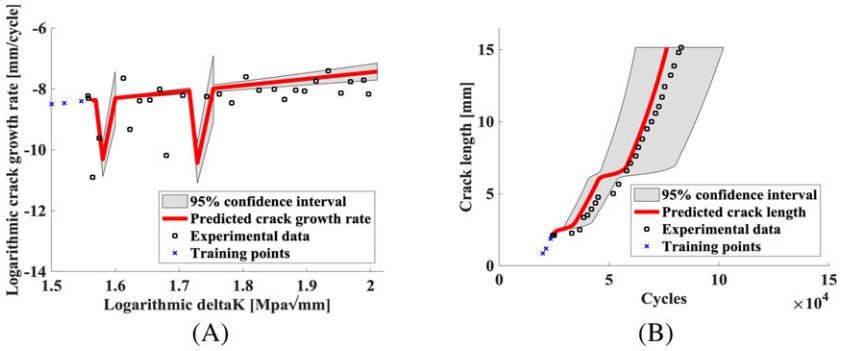

FIGURE 13 Predictions of the crack growth rate and crack propagation with an overload ratio of 1.75 and the scenario of two overloads in a single test [Colour figure can be viewed at wileyonlinelibrary.com]

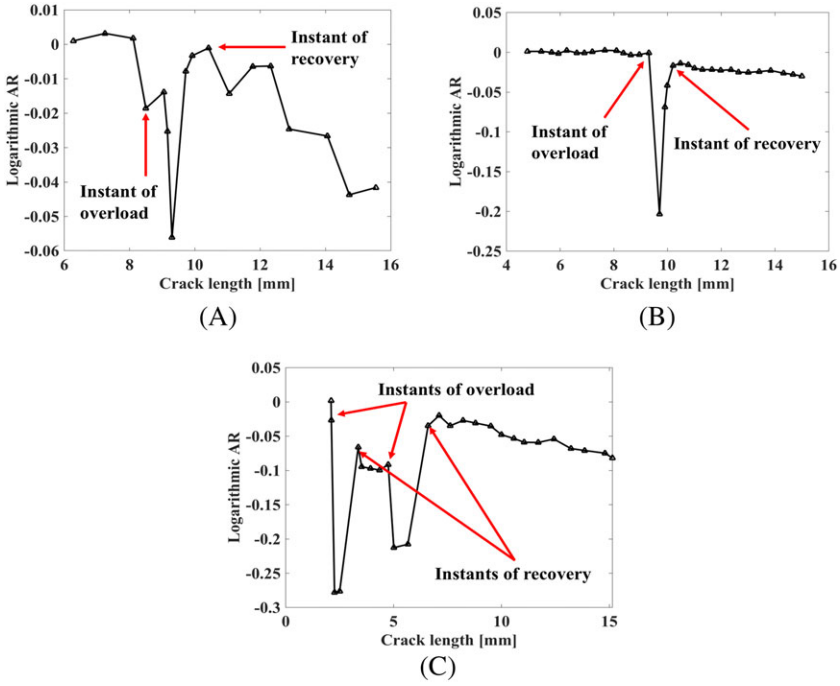

FIGURE 14 Logarithmic AR propagation with respect to crack length in the tests: A, overload ratio of 1.75, five training points, $\Delta a = 0.01$ and one overload in a single test; B, overload ratio of 2.0, five training points, $\Delta a = 0.01$ and one overload in a single test; C, overload ratio of 1.75, three training points, $\Delta a = 0.01$ and two overloads in a single test [Colour figure can be viewed at wileyonlinelibrary.com]

crack length. The purpose of this study is to assess the long-term prediction capability as well as to explore potential directions that can improve the performance of the developed model. Before discussing the error propagation, it is necessary to mention the potential consequences of underprediction and overprediction in this study. When the developed model undergoes an underprediction, an unnecessary maintenance decision may be suggested, because the predicted crack at a future instant is larger than it would be, resulting in extra maintenance cost. When the developed model experiences an overprediction, the risk of structural failure significantly increases because the predicted crack at a future instant is less severe than it would be, resulting in unexpected loss of structural functionality. Based on these definitions, the overprediction seems to be a much more dangerous scenario for a decision-making system.

Figure 14A to C presents the logarithmic AR propagation with respect to crack length in three aforementioned testing examples. As presented in Equation 14, a small absolute value of logarithmic AR indicates a precise prediction of the developed model. Recalling the definition of AR, a positive AR indicates an overprediction ($N_f > (N_{gt})_f$) and a negative AR indicates an underprediction ($N_f < (N_{gt})_f$). It is seen that there is no significant overprediction in these three cases; most errors are underpredictions, which may prevent the model from an unexpected failure. Two observations need to be discussed here: First, when comparing with the predicted crack growth far away from the overload, the predictions between the instants of overload and recovery have relatively larger errors. The reason is that the behavior of crack propagation immediately after an overload is very complex, and its nonlinearity is not fully explored by the offline model using very limited amount of training points. The prediction accuracy of the developed model is expected to be improved if a larger amount of training examples is provided to the offline model. Second, after the overload, the negative logarithmic AR keeps decreasing with respect to the crack length, indicating that the underprediction error increases as distance between the predicted point and first few training points increases. The interpretation is that the overload has an impact on the crack growth even after the instant of recovery; this impact slows down the crack propagation and results in an increase in underprediction error with respect to the crack length after overload. Even if the prediction of the developed model is very accurate, this observation suggests that the accuracy of this model can be further improved by including an additional variable in the offline model to compensate for the impact of overload on the later stages of crack growth under constant loading.

5 | CONCLUDING REMARKS

An online-offline model was developed for accurately predicting the crack propagation under biaxial in-phase loading conditions with overload. The online model intelligently combined a physics-based finite element model with a Gaussian process based data-driven prognosis model; the offline model was trained by the defined physics-based parameters including the minimum crack

growth rate, crack growth retardation rate, and crack growth acceleration rate, which were obtained from existing experiments, and used to inform the online model for the prediction of crack propagation behaviors after the instant of overload. The developed model was then validated by three experiments using aluminum AA7075-T651 alloy with varying overload ratios and number of overload instances in a single overload; the predicted crack behavior showed a good agreement with the actual tests including the crack retardation due to the presence of overload. The sensitivities of the number of training points and crack increment Δa to prediction accuracy were evaluated by investigating the MAPE of each case. Lastly, the logarithmic AR was used to study the propagation of prediction error with respect to the crack length, indicating that the presence of overload had an impact on the crack propagation even after crack growth rate fully recovered. This suggests that an additional variable could be included in the offline model to improve the accuracy of the developed model in predicting long-term crack propagation after overloads.

ACKNOWLEDGEMENTS

This research was sponsored by the US Navy Naval Air Systems Command and Technical Data Analysis Inc., prime contract #N68335-16-G-0009, DO 0001, Program managers Dr Nam Phan and Dr Nagaraja Iyyer.

ORCID

Guoyi Li https://orcid.org/0000-0002-9228-4236

REFERENCES

1. Sakai T. Review and prospects for current studies on very high cycle fatigue of metallic materials for machine structural use. *J Solid Mech Mater Eng*. 2009;3(3):425-439.
2. Ewing JA, Humfrey JC. The fracture of metals under repeated alternations of stress. *Proc Roy Soc Lond A*. 1903;71(467–476):79-97.
3. Vecchio1 RS, Hertzberg RW, Jaccard2 R. On the overload induced fatigue crack propagation behavior in aluminum and steel alloys. *Fatigue Fract Eng Mater Struct*. 1984;7(3):181-194.
4. Borrego LP, Ferreira JM, Costa JM. Fatigue crack growth and crack closure in an AlMgSi alloy. *Fatigue Fract Eng Mater Struct*. 2001;24(4):255-265.
5. Sunder R, Andronik A, Biakov A, Eremin A, Panin S, Savkin A. Combined action of crack closure and residual stress under periodic overloads: a fractographic analysis. *Int J Fatigue*. 2016;82:667-675.
6. Chen G, Chen X, Niu CD. Uniaxial ratcheting behavior of 63Sn37Pb solder with loading histories and stress rates. *Mater Sci Eng A*. 2006;421(1–2):238-244.
7. Schaff JR, Davidson BD. Life prediction methodology for composite structures. Part I—constant amplitude and two-stress level fatigue. *J Thermoplast Compos Mater*. 1997;31(2):128-157.
8. Colin J, Fatemi A. Variable amplitude cyclic deformation and fatigue behaviour of stainless steel 304L including step, periodic, and random loadings. *Fatigue Fract Eng Mater Struct*. 2010;33(4):205-220.
9. Hopper CD, Miller KJ. Fatigue crack propagation in biaxial stress fields. *J Strain Anal Eng Des*. 1977;12(1):23-28.
10. Anderson PR, Garrett GG. Fatigue crack growth rate variations in biaxial stress fields. *Int J Fract*. 1980;16(3):R111-R116.
11. Sunder R, Ilchenko BV. Fatigue crack growth under flight spectrum loading with superposed biaxial loading due to fuselage cabin pressure. *Int J Fract*. 2011;33(8):1101-1110.
12. Perel VY, Misak HE, Mall S, Jain VK. Biaxial fatigue crack growth behavior in aluminum alloy 5083-H116 under ambient laboratory and saltwater environments. *J Mater Eng Perform*. 2015;24(4):1565-1572.
13. Datta S, Chattopadhyay A, Iyyer N, Phan N. Fatigue crack propagation under biaxial fatigue loading with single overloads. *Int J Fatigue*. 2018;109:103-113.
14. Datta S, Chattopadhyay A. Micromechanisms governing crack propagation in Al 7075 under in-plane biaxial fatigue with single overloads. In2018 AIAA/ASCE/AHS/ASC Structures, Structural Dynamics, and Materials Conference 2018 (p. 2004).
15. Neerukatti RK, Datta S, Chattopadhyay A, Iyyer N, Phan N. Fatigue crack propagation under in-phase and out-of-phase biaxial loading. *Fatigue Fract Eng Mater Struct*. 2018;41(2):387-399.
16. Arcari A, Apetre N, Dowling N, et al. Variable amplitude fatigue life in VHCF and probabilistic life predictions. *Procedia Engineering*. 2015;114:574-582.
17. Liu Y, Venkatesan KR, Zhang W. Time-based subcycle formulation for fatigue crack growth under arbitrary random variable loadings. *Eng Fract Mech*. 2017;182:1-8.
18. Ray A, Patankar R. Fatigue crack growth under variable-amplitude loading: part I—model formulation in state-space setting. *App Math Model*. 2001;25(11):979-994.
19. Ray A, Patankar R. Fatigue crack growth under variable-amplitude loading: part II—code development and model validation. *App Math Model*. 2001;25(11):995-1013.
20. Kiran R, Khandelwal K. A micromechanical cyclic void growth model for ultra-low cycle fatigue. *Int J Fatigue*. 2015;70:24-37.
21. Neerukatti RK, Liu KC, Kovvali N, Chattopadhyay A. Fatigue life prediction using hybrid prognosis for structural health monitoring. *J Aerosp Inf Syst*. 2014;11(4):211-232.
22. Neerukatti RK, Chattopadhyay A, Iyyer N, Phan N. A hybrid prognosis model for predicting fatigue crack propagation under biaxial in-phase and out-of-phase loading. *Struct Health Monit*. 2018;17(4):888-901.
23. Williams CK, Rasmussen CE. Gaussian processes for machine learning. *The MIT Press*. 2006;2(3):4.
24. Hyndman RJ, Koehler AB. Another look at measures of forecast accuracy. *Int J Forecast*. 2006;22(4):679-688.

25. Tofallis C. A better measure of relative prediction accuracy for model selection and model estimation. *J Oper Res Soc*. 2015;66(8):1352-1362.
26. Morley SK, Brito TV, Welling DT. Measures of model performance based on the log accuracy ratio. *Space Weather*. 2018;16(1):69-88.
27. Hibbett, Karlsson, Sorensen. ABAQUS/standard: User's Manual. Hibbitt, Karlsson & Sorensen; 1998.
28. Aksoy S, Haralick RM. Feature normalization and likelihood-based similarity measures for image retrieval. *Pattern Recogn Lett*. 2001;22(5):563-582.

How to cite this article: Li G, Datta S, Chattopadhyay A, Iyyer N, Phan N. An online-offline prognosis model for fatigue life prediction under biaxial cyclic loading with overloads. *Fatigue Fract Eng Mater Struct*. 2019;42:1175–1190. https://doi.org/10.1111/ffe.12983